

# Computational Fluid Dynamics Study on Water Soot Blower Direction in Tangentially Fired Pulverized-Coal Boiler

Teewin Plangsrinont, Wasawat Nakkiew

**Abstract**—In this study, Computational Fluid Dynamics (CFD) was utilized to simulate and predict the path of water from water soot blower through an ambient flow field in 300-megawatt tangentially burned pulverized coal boiler that utilizes a water soot blower as a cleaning device. To predict the position of the impact of water on the opposite side of the water soot blower under identical conditions, the nozzle size and water flow rate were fixed in this investigation. The simulation findings demonstrated a high degree of accuracy in predicting the direction of water flow to the boiler's water wall tube, which was validated by comparison to experimental data. Results show maximum deviation value of the water jet trajectory is 10.2%.

**Keywords**—Computational fluid dynamics, tangentially fired boiler, thermal power plant, water soot blower.

## I. INTRODUCTION

TANGENTIALLY fired boilers are the most widely used in the power generation industry. At the tangentially burned boiler, the fuel and air are injected from the burners arranged and adjusted to generate a concentric whirling fireball in the furnace's center [1].

Mae Moh power plant is a pulverized-coal-fired power plant designed to burn low quality lignite [2]. It consists of seven generators with the total generating capacity of 2,455 megawatts, including six 300-megawatt units and one 655-megawatt unit. For 300-megawatt unit pulverized coal boilers, slag is generated during the combustion process and accumulates on the water wall tube, reducing the boiler's efficiency. As a result, steam soot blowers and water soot blowers were installed to remove slag from the water wall tube [3].

Water Soot blower (WSB) is another cleaning device in the furnace that receives a cleaning signal from the temperature sensor on the other wall and then generates a water jet through the furnace to the opposite water wall tube for cleaning slag, as shown in Fig. 1.

The issue with the WSB is the trajectory prediction of the water jet since the vast scale of the boiler necessitates a lengthy setup process. Additionally, testing must be carried out during shutdown periods which has a challenging condition and limited time

T. Plangsrinont is with Electricity Generating Authority of Thailand (EGAT), Graduate Program in Industrial Engineering, Faculty of Engineering, Chiang Mai University, Thailand (phone: +66-54-253231; fax: +66-54-253238; e-mail: teewin.p@egat.co.th).

W. Nakkiew, is with Department of Industrial Engineering, Faculty of Engineering, Chiang Mai University.



Fig. 1 Water jet from WSB

CFD is a useful tool and widely used in power plant investigation to predict the fluid flow. The influence of tilt angles on flow and combustion will be investigated in a 120-megawatt industrial boiler using a CFD model to depict the temperature and velocity distribution [4], and in a pulverized coal utility boiler using CFD simulation to demonstrate the behavior of flow following jet burners [5]. CFD was utilized in this work to develop a model of a WSB as a prototype for predicting the trajectory of a water jet in a coverage cleaning area by using the volume of fluid (VOF) method with 10,000,000 tetrahedral cells. To simplify the problem, we assume that all processes are in steady-state and the temperature has no influence.

## II. METHOD

### A. Model

The schematic diagram of the boiler is shown in Fig. 2. All dimensions necessary to produce the geometry model are taken from the plant boiler handbook and include a width of 13.83 meters, a depth of 15.32 meters, and a height of 67.92 meters. WSB and temperature sensor are positioned at the boiler's front water wall tube at an elevation of 30.32 meters and at the boiler's rear water wall tube at an elevation of 30.780 meters, respectively.

The investigation domain is depicted in Fig. 3 which is the portion of the coverage area for WSB cleaning from the front water wall tube to the rear water wall tube. The geometry model employs the WSB as the inquiry domain's central point, which is positioned on the front water wall tube and set to (0, 0, 0) in Cartesian Coordinates (x, y, z) in the meter unit. For coverage, the cleaning area boundary includes an upper and lower limit of 5 m to -5 m in the y-axis, a left and right limit of 7.505 m to -7.808 m in the x-axis, a distance of 0 m to 13.83

m between the front and rear water wall tubes, and a temperature sensor situated on the rear water wall tube at (2.26, 0.46, 13.83) The examination domain from the rear side perspective is shown in Fig. 4, and the Cartesian Coordinates are shown in Table I.

TABLE I  
DETAILED OF CARTESIAN COORDINATE

Description	Quantity
WSB	(0, 0, 0)
Temperature Sensor	(2.26, 0.46, 13.83)
Point 1	(-7.808, 5.000, 13.830)
Point 2	(7.508, 5.000, 13.830)
Point 3	(-7.808, -5.000, 13.830)
Point 4	(7.508, -5.000, 13.830)

**B. Governing Equations**

To ensure that the simulation results are accurate, the geometric model, mesh, boundary conditions, numerical method, and convergence criteria are all considered. In a numerical simulation of a 1000-megawatt tangentially burned tower-type boiler at full size, a high-quality mesh of 4,130,000 hexahedral cells was used [6]. CFD simulations in a domain of 10,000,000 tetrahedral cells were used in this work to predict the trajectory of a water jet in a coverage cleaning area.

Reynolds-averaged Navier–Stokes equations (RANS) are time-averaged fluid flow equations. The equations are based on the concept of Reynolds decomposition, which divides an instantaneous variable into its time-averaged and fluctuating components. Generally, the RANS equations are used to describe turbulent flows. These equations can be used to

estimate time-averaged solutions to the Navier–Stokes equations using knowledge of the features of flow turbulence. These equations are stated in Einstein notation in Cartesian coordinates for a stationary flow of an incompressible Newtonian fluid as:

$$\rho \bar{u}_j \frac{\partial \bar{u}_i}{\partial x_j} = \frac{\partial}{\partial x_i} \left[ -\bar{p} \delta_{ij} + \mu \left( \frac{\partial \bar{u}_i}{\partial x_j} + \frac{\partial \bar{u}_j}{\partial x_i} \right) - \rho \overline{u'_i u'_j} \right] \quad (1)$$

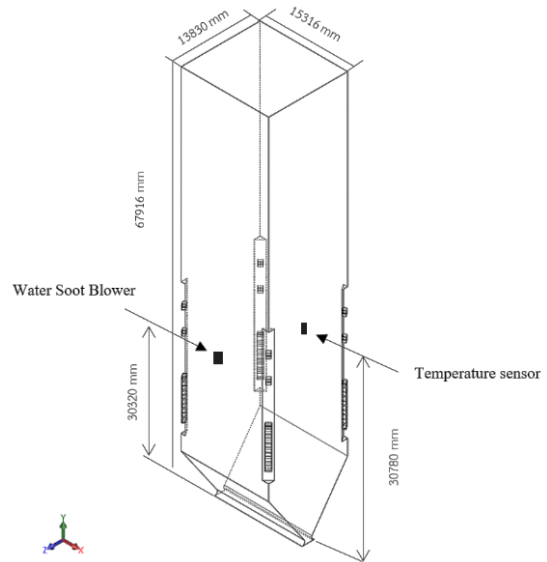


Fig. 2 Schematic diagram of the boiler

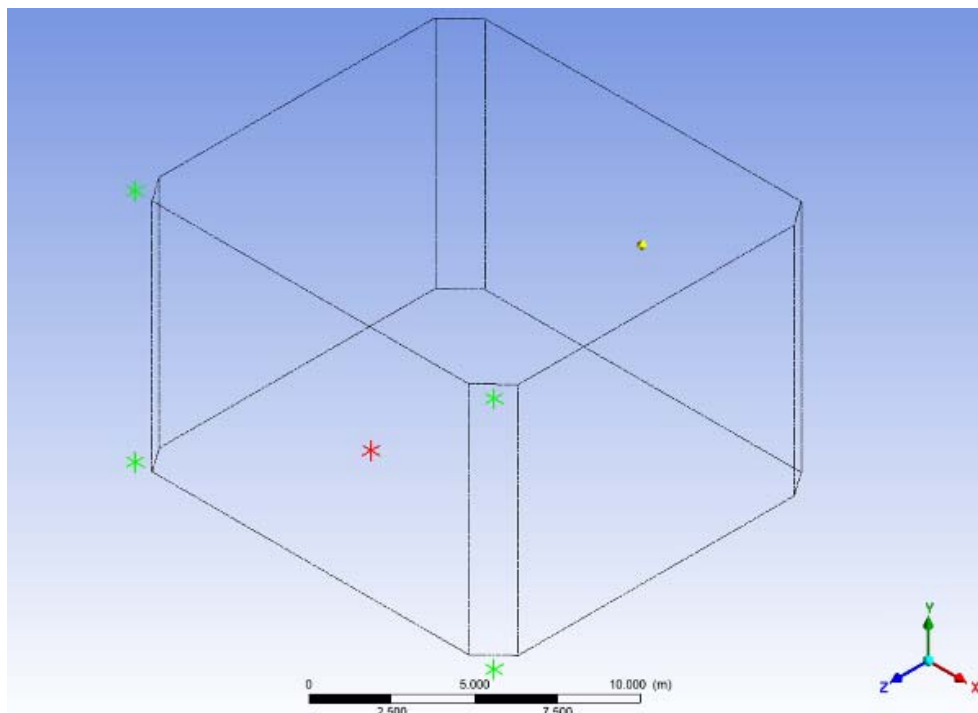


Fig. 3 The investigation domain

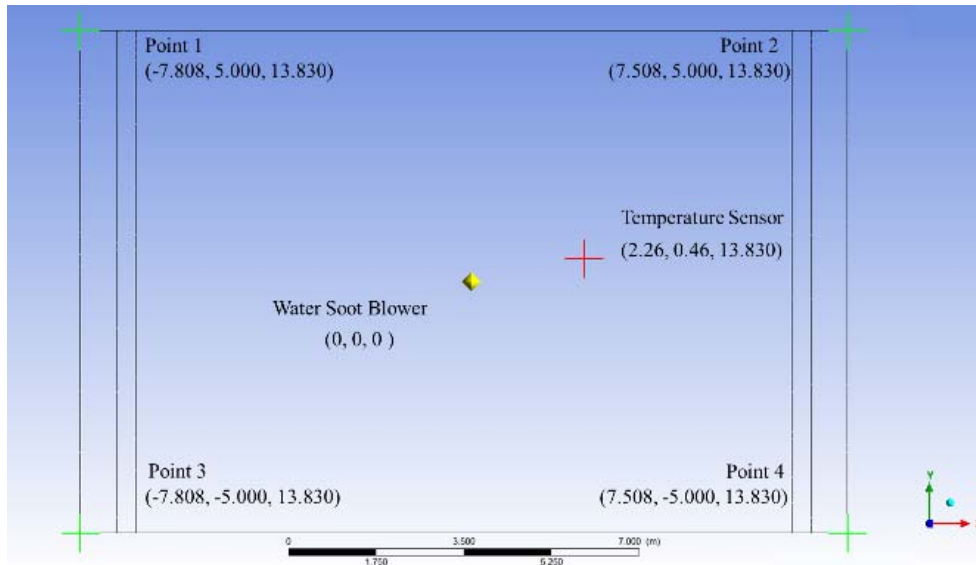


Fig. 4 Investigation domain at rear side view

The left-hand side of (1) denotes the change in mean momentum of a fluid element caused by mean flow unsteadiness and convection caused by mean flow. The mean body force, the isotropic stress due to the mean pressure field, the viscous stresses ( $\rho \overline{u_i' u_i'}$ ) due to the changing velocity field, together referred to as the Reynolds stress, all contribute to balancing this shift. This nonlinear Reynolds stress element needs extra modeling in order to solve the RANS equation, which has resulted in the development of several turbulence models.

In the CFD model, there are several options for a turbulence model. One of turbulence used as an alternative model is Re-Normalization Group (RNG)  $k-\epsilon$  model [7], [8]. This model is known for predicting residual swirls and reliable for a wider class of flows than the standard  $k-\epsilon$  model. It is similar in form to the standard  $k-\epsilon$  model but The RNG model has an additional term in its  $\epsilon$  equation that significantly improves the accuracy. The RNG theory provides an analytical formula for turbulent Prandtl numbers, while the standard  $k-\epsilon$  model uses user-specified, constant values.

This study uses the RNG  $k-\epsilon$  for the turbulence model. The RNG-based  $k-\epsilon$  turbulence model is derived from the instantaneous Navier-Stokes equations, using a mathematical technique called "renormalization group" (RNG) methods.

Transport equations for the RNG  $k-\epsilon$  model are the analytical derivation, result in a model with constants different from those in the standard  $k-\epsilon$  model, and additional terms and functions in the transport equations for  $k-\epsilon$  model (2), (3).

$$\frac{\partial}{\partial t}(\rho k) + (\rho k u_i) = \frac{\partial}{\partial x_i} \left( \alpha_i u_{eff} \frac{\partial k}{\partial x_i} \right) + G_k + G_b - \rho \epsilon - Y_u + S_k \quad (2)$$

and,

$$\frac{\partial}{\partial t}(\rho \epsilon) + \frac{\partial}{\partial x_i}(\rho \epsilon u_i) = \frac{\partial}{\partial x_i} \left( \alpha_i u_{eff} \frac{\partial \epsilon}{\partial x_i} \right) + C_{1\epsilon} \frac{\epsilon}{k} (G_k + C_{3\epsilon} G_b) - C_{2\epsilon} \rho \frac{\epsilon^2}{k} - R_\epsilon + S_\epsilon \quad (3)$$

$G_k$  represents the generation of turbulence kinetic energy due to the mean velocity gradients,  $G_b$  is the generation of turbulence kinetic energy due to buoyancy,  $Y_m$  represents the contribution of the fluctuating dilatation in compressible turbulence to the overall dissipation rate, The quantities  $\alpha_k$  and  $\alpha_\epsilon$  are the inverse effective Prandtl numbers for  $k$  and  $\epsilon$ , respectively.  $S_k$  and  $S_\epsilon$  are user-defined source terms.

The VOF model is used to track the volume fraction of each of the fluids throughout the domain. Typical applications include the prediction of the motion of liquid and the steady or transient tracking of any liquid-gas interface. All fluids use the same single set of momentum equations. The volume fraction of each fluid is tracked through every cell in the computational grid. When a cell is empty with no traced fluid inside, the value of  $C$  is zero; when the cell is full,  $C = 1$ ; and when there is a fluid interface in the cell,  $0 < C < 1$ . The evolution of the  $m$ -th fluid in a system on  $n$  fluids is governed by the transport equation.

$$\frac{\partial C_m}{\partial t} + v \cdot \nabla C_m = 0, \quad (4)$$

with the following constraint,

$$\sum_{m=1}^n C_m = 1, \quad (5)$$

The VOF remains constant. For each cell property, such as density  $\rho$ , it is calculated by the volume fraction average of

the total fluid in the cell.

$$\rho = \sum_{m=1}^n \rho_m C_m \quad (6)$$

### C. Boundary Conditions

The boundary conditions for simulation are obtained from the WSB operation. The dimensions of the boiler correspond to the drawings in the boiler handbook. The water jet is generated by the WSB using a multiphase flow of air and water. The nozzle's water flow rate is 10 kg/s and nozzle size is 14.00 mm. The constant number for turbulence RNG k-model C1-epsilon is 1.42, whereas C2-epsilon is 1.68. The constant value of turbulence RNG k-ε model  $c_{1\epsilon}$  and  $c_{2\epsilon}$  is listed in Table II.

TABLE II  
BOUNDARY CONDITIONS

Boiler Width (Distance from Nozzle to Sensor)	13.83 m
Boiler Depth	15.32 m
Boiler height	67.92 m
Elevation of WSB	30.32 m
Elevation of Temperature Sensor#	30.78 m
Water flow rate	10.00 kg/s
Nozzle size	14.00 mm
$c_{1\epsilon}$	1.42
$c_{2\epsilon}$	1.68

### III. EXPERIMENT

The WSB trajectory experiment was conducted during the shutdown period. To conduct the experiment, a temperature sensor was mounted on the exterior of the boiler's back wall tube to act as a detection target when the water jet hits, as seen in Fig. 5. That is because while the boiler is in operation, the temperature on the water wall is high and decreases when water hits the sensor. However, during the maintenance shutdown, the boiler was cooled down, and both the temperature at the wall tube and the ambient air temperature were low. As a result, the temperature sensor was unable to detect temperature changes. To resolve this issue, a heater was employed to raise the temperature at the sensor, allowing the target to be distinguished when the water jet struck the sensor.

The WSB was controlled by motion control software to regulate the horizontal and vertical direction of the water jet flow from the motor module. Maximum movement distance in the horizontal and vertical path was from 0-230 mm to cover the cleaning area. When the WSB was operating, water was going across the boiler from the front to the back of the water wall tubes. Then the trajectory direction of WBS has adjusted the motion along the axis to find the coordinate that hit the sensor as show in Fig. 6.

When the water jet hits the temperature sensor, the sensor's temperature changed. In this setting, the temperature sensor was heated to 80 °C and the WSB operated for 30 seconds each test. Then, the drive module was moved horizontally and vertically to determine the location of the drive module that

caused the greatest difference in temperature sensor readings.

The optimal condition for determining the water jet impact target point was when the data logger recorded the most distinct temperature and spent the least amount of time transitioning to steady-state. The result indicated that the most distinct temperature was 35 °C and the least amount of time transitioning to steady-state was 20 seconds. At the drive module, the horizontal and vertical distances were 0.260 mm and 0.027 mm, respectively, as seen in Fig. 7.#



Fig. 5 Temperature sensor and heater installation



Fig. 6 WSB in testing

### IV. RESULT AND DISCUSSION

The result of the velocity distribution of the water jet trajectory from the CFD model is shown in Fig. 8. The dot on the investigative domain represents the location of the temperature sensor and the trajectory of the water jet hit, respectively. A soot blower creates a water jet that passes from the front wall tube to the back wall tube. The end of the water jet's trajectory indicates a hit point near the temperature sensor.

The temperature sensor is located on Cartesian Coordinates (x, y, z) at (2.26, 0.46, 13.83) m in the Y-X plane, and the trajectory of the water jet impacts the rear water wall tube on Cartesian Coordinates (3.57, -0.56, 13.83) m in the Y-X plane, as illustrated in Fig. 9.

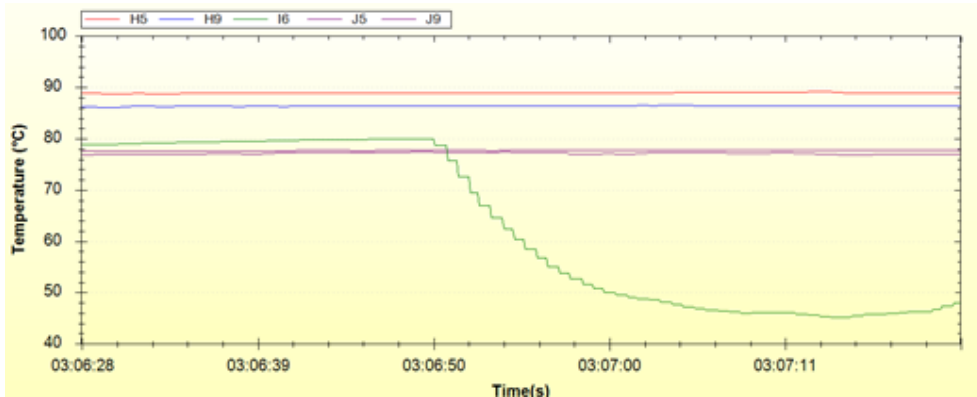


Fig. 7 Different temperature data from data logger

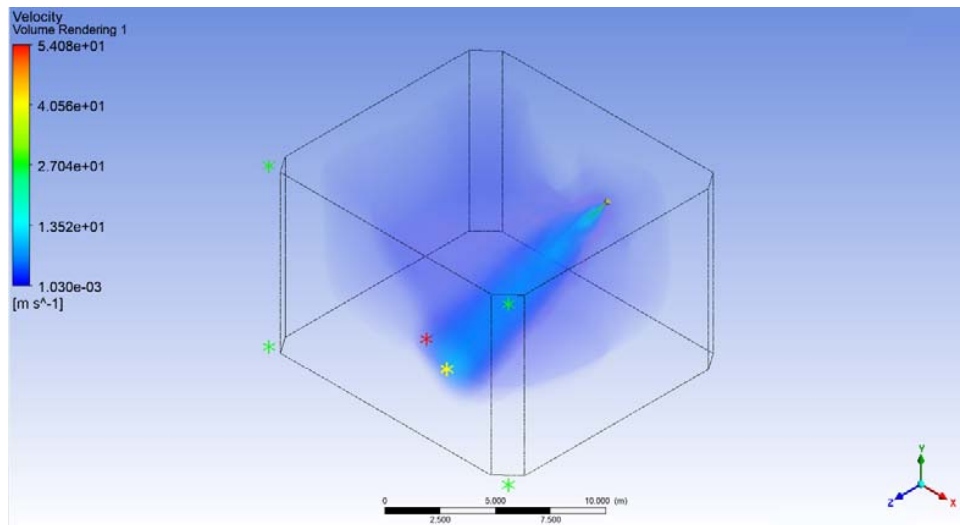


Fig. 8 Velocity distribution in investigation domain

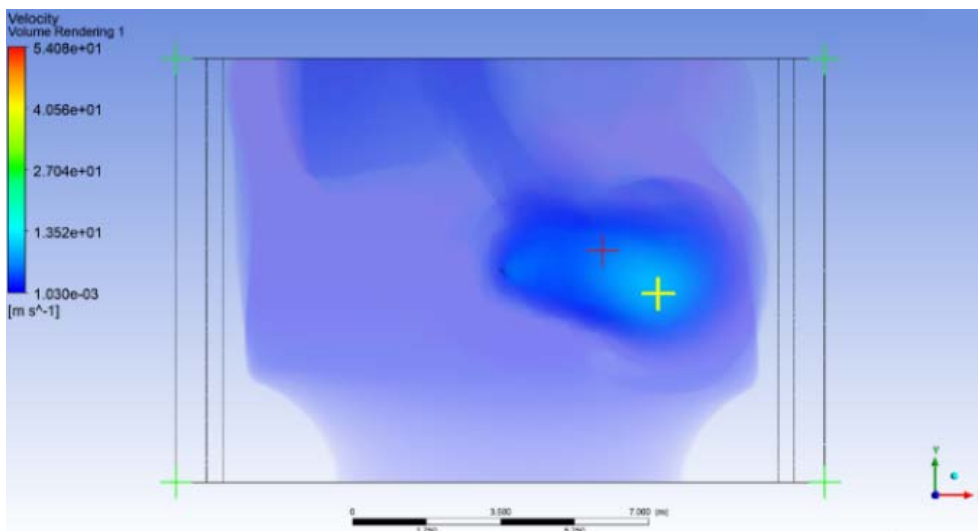


Fig. 9 Trajectory of water jet impact the rear waterwall tube

On the Y-Z plane, at Cartesian Coordinate  $z = 13.83$  m, the temperature sensor is located at  $0.46$  m on the Cartesian

Coordinate in the Y-axis, and the trajectory of the water jet impacts the rear water wall tube at  $-0.56$  m, or an absolute

distance of 1.02 m, as seen in Fig. 10.

In comparison to a WSB, the maximum coverage cleaning

area along the Y-axis is 10.00 m. The conclusion of the CFD model deviates by 10.2% from the experiment.

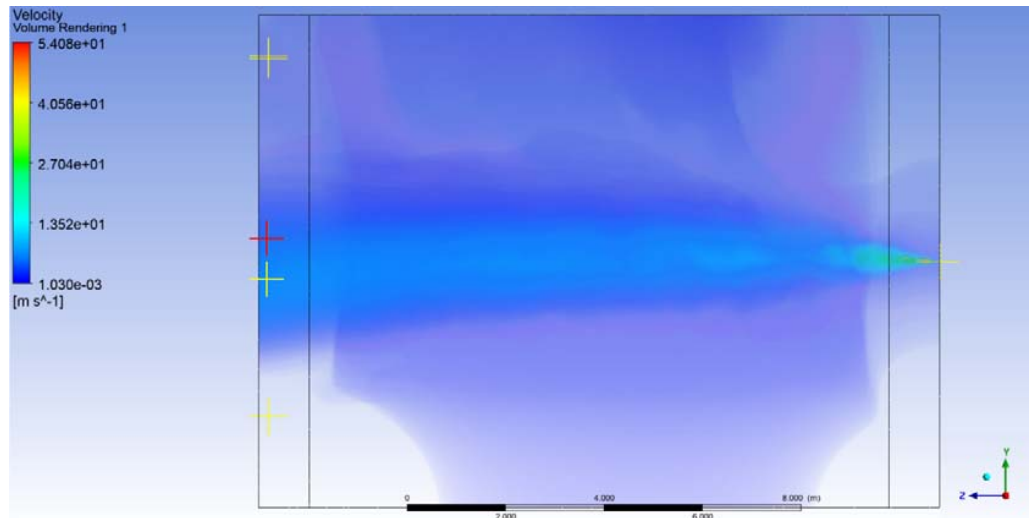


Fig. 10 Trajectory of water jet in the Y-Z plane

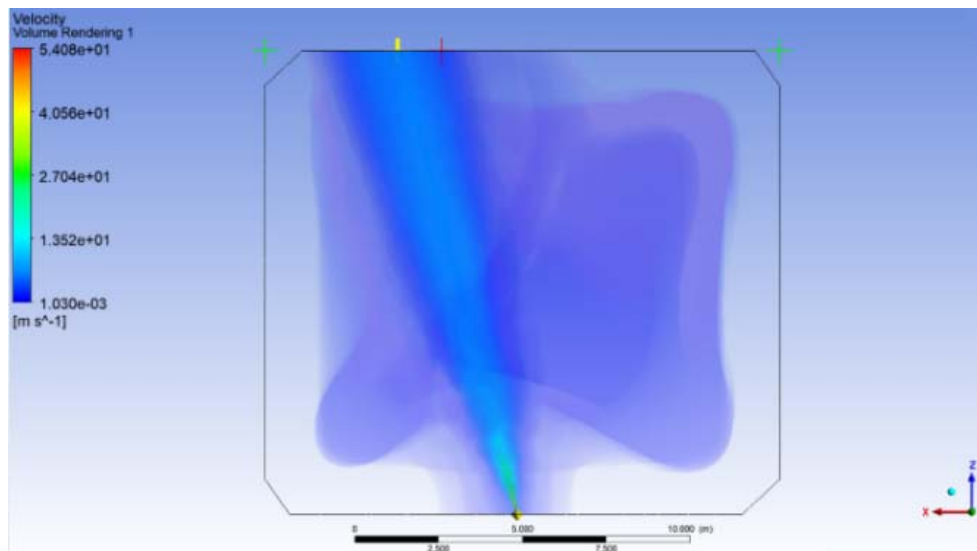


Fig. 11 Trajectory of water jet in the Z-X plane

In the Z-X plane, at Cartesian Coordinate  $z = 13.83$  m, the temperature sensor is located at 2.26 m along the X-axis, and the trajectory of the water jet impacts the rear water wall tube at 3.57 m along the X-axis, or an absolute distance of 1.31 m, as shown in Fig. 11.

In comparison to a WSB, the maximum coverage cleaning area along the Y-axis is 15.32 m. The conclusion of the CFD model deviates by 8.55% from the experiment.

## V. CONCLUSION

When compared to experimental data, the CFD model produced accurate predictions of the trajectory of water jet. For the deviation values of the water jet trajectory and the

experimental values, the covering cleaning area is 10.2% on the Y-axis and 8.55% on the X-axis.

## ACKNOWLEDGMENT

This research is supported by EGAT-CMU scholar program of Electricity Generating Authority of Thailand (EGAT) and Chiang Mai University (CMU).

## REFERENCES

- [1] Pintana P., Tippayawong N., "Predicted formation and deposition of slag from lignite combustion on pulverized coal boilers," International Conference on Chemical Engineering and Materials Science (CEMS'14), vol. 10, pp. 202-210, March 2014.
- [2] Dengfeng T., Lijin Z., Peng T., Lun M., Qingyan F., Cheng Z., Dianping Z., Gang C. "Influence of vertical burner tilt angle on the gas

- temperature deviation in a 700 MW low NO<sub>x</sub> tangentially fired pulverized-coal boiler,” *Fuel Processing Technology* 138, pp. 616-628, July 2015.
- [3] Partch K., “Stress Analysis of Water Wall Tubes of a Coal-fired Boiler during Soot Blowing Operation,” *World Academy of Science, Engineering and Technology International Journal of Mechanical and Mechatronics Engineering* vol. 10, no. 3, 2016.
- [4] Wisam S. A., Hasril H., Zamri Y., “CFD Investigation of the effect of tilt angles to flow and combustion in a 120 Mw Gas-Fired full scale industrial boiler,” *International Journal of Scientific & Technology Research*, vol. 4, issue 12, December 2015.
- [5] Norbert M., “Computational modeling of a utility boiler tangentially-fired furnace retrofitted with swirl burners,” *Fuel Processing Technology* 91, pp. 1601-1608, June 2010.
- [6] Peng T., Qingyan F., Sihan Z., Chungen Y., Cheng Z., Haibo Z., Gang C., “Causes and mitigation of gas temperature deviation in tangentially fired tower-type boilers,” *Applied Thermal Engineering* 139, pp. 135-143, 2018.
- [7] Bhargav A., Jaesool S., Kisoo Y., “Numerical and experimental study on biased tube temperature problem in tangential firing boiler” *Applied Thermal Engineering* 126, pp. 92-99, July 2017.
- [8] Choeng R. C., Chang N. K., “Numerical investigation on the flow, combustion and NO<sub>x</sub> emission characteristics in a 500 MWe tangentially fired pulverized-coal boiler”, *Fuel* vol. 88, issue 9, pp. 1720-1731, April 2009.